HHS Public Access

Author manuscript

Biochem J. Author manuscript; available in PMC 2015 May 18.

Published in final edited form as:

Biochem J. 2013 July 15; 453(2): 209–218. doi:10.1042/BJ20121126.

MondoA senses adenine nucleotides: transcriptional induction of thioredoxin-interacting protein

Kyoung-Sim Han and **Donald E. Ayer**[1]

Department of Oncological Sciences, Huntsman Cancer Institute, University of Utah, Salt Lake City, UT 84112, U.S.A.

Abstract

The MondoA–Mlx transcription complex plays a pivotal role in glucose homoeostasis by activating target gene expression in response to G6P (glucose 6-phosphate), the first reaction intermediate in glycolysis. TXNIP (thioredoxin-interacting protein) is a direct and glucose-responsive target of MondoA that triggers a negative-feedback loop by restricting glucose uptake when G6P levels increase. We show in the present study that TXNIP expression is also activated by AICAR (5-amino-4-imidazolecarboxamide ribofuranoside) and adenosine. Using pharmacological inhibitors and genetic knockdowns of purine metabolic enzymes, we establish that TXNIP induction by AICAR and adenosine requires their cellular uptake and metabolism to adenine nucleotides. AICAR induction of TXNIP depended on MondoA, but was independent of AMPK (AMP-activated protein kinase) activation and calcium. The findings of the present study have two important implications. First, in addition to activating AMPK, AICAR may have AMPK-independent effects on gene expression by regulating MondoA–Mlx activity following its flux into the adenine nucleotide pool. Secondly, MondoA–Mlx complexes sense elevated levels of G6P and adenine nucleotides to trigger a TXNIP-dependent feedback inhibition of glycolysis. We propose that this mechanism serves as a checkpoint to restore metabolic homoeostasis.

Keywords

adenine nucleotide; 5-amino-4-imidazolecarboxamide ribofuranoside (AICAR); bioenergetics; glucose metabolism; MondoA; thioredoxin-interacting protein (TXNIP)

INTRODUCTION

Cells maintain energy homoeostasis by responding to changes in nutrient status [1]. Glucose is a fundamental nutrient, providing ATP for energy as well as carbon for biosynthesis [2]. Defects in glucose sensing and metabolism can lead to the development of insulin resistance and Type 2 diabetes [3]. Furthermore, a common feature of tumour cells is a higher dependence on aerobic glycolysis for their energy needs rather than a dependence on

[1] To whom correspondence should be addressed (Don.Ayer@hci.utah.edu)..

AUTHOR CONTRIBUTION

Kyoung-Sim Han performed the experiments and data analysis. Kyoung-Sim Han and Donald Ayer designed the research and wrote the paper.

OXPHOS (oxidative phosphorylation) [4]. Given these pleiotropic roles for glucose in energy homoeostasis, tight regulation of glucose metabolism is absolutely required for normal cell physiology.

The MondoA transcription factor is a master regulator of glucose-responsive transcription [5]. MondoA is a member of the bHLHZip (basic helix–loop–helix leucine zipper) transcription factor family and forms heterodimeric complexes with another bHLHZip protein, Mlx [6]. MondoA–Mlx complexes reside at the OMM (outer mitochondrial membrane) and shuttle between the OMM and the nucleus when glucose levels are low [7]. MondoA–Mlx complexes accumulate in the nucleus and bind to ChoREs (carbohydrate-response elements) in the promoters of target genes in response to increased glycolytic flux [5]. G6P (glucose 6-phosphate), promotes MondoA transcriptional activity by regulating nuclear accumulation, promoter occupancy and coactivator recruitment [8].

Our previous studies identified TXNIP (thioredoxin-interacting protein) as a direct and glucose-responsive target of MondoA–Mlx complexes [5,8,9]. TXNIP binds to thioredoxin and inhibits its disulfide reductase activity, regulating the cellular redox state [10]. However, TXNIP plays a broader multifunctional role by regulating diverse cellular phenomenon [11]. One such role is as a critical regulator of glucose metabolism by negatively regulating glucose uptake [12,13]. TXNIP expression is robustly induced by glucose through a ChoRE in its promoter [14]. MondoA binds directly to the ChoRE in the *Txnip* promoter following glucose stimulation and TXNIP expression is reduced or virtually eliminated by knockdown of MondoA or genetic deletion [5,8,9,15,16]. ARRDC4 (arrestin domain-containing protein 4), a TXNIP paralogue, is also glucose-induced and a direct target of MondoA [5,8]. The function of ARRDC4 remains unclear, but, like TXNIP, it inhibits glucose uptake [13]. Consistent with the roles of TXNIP and ARRDC4 as negative regulators of glucose uptake and MondoA target genes, MondoA knockdown or knockout results in increased glucose uptake [5,8,9,16]. Therefore MondoA–Mlx complexes drive feedback inhibition of glucose uptake by activating target gene expression when G6P levels are excessively high. Thus MondoA functions as a glucose sensor and triggers an adaptive transcriptional response to high glycolytic flux.

AMPK (AMP-activated protein kinase) is a sensor of intracellular bioenergetics. AMPK is activated by low bioenergetic charge, such as high AMP levels, and activates numerous catabolic pathways to restore energy homoeostasis [17]. AICAR (5-amino-4-imidazolecarboxamide ribofuranoside) is commonly used to activate AMPK. AICAR is an adenosine analogue that is phosphorylated by ADK (adenosine kinase) to yield ZMP (5-amino-4-imidazolecarboxamide ribonucleotide; AICAR monophosphate). ZMP activates AMPK by mimicking the effects of AMP on AMPK and the upstream AMPK kinase LKB1/STK11 (serine/threonine kinase) [18]. AICAR also has anti-inflammatory, pro-apoptotic and pro-differentiation effects that are AMPK-independent. For example, AICAR suppresses LPS (lipopolysaccharide)-induced inflammation in macrophages by inhibiting the production of pro-inflammatory cytokines [19–21]. AICAR induces apoptosis by activating caspases and cytochrome *c* release in T-lymphoblasts [22,23] and facilitates apoptosis induced by TRAIL [TNF (tumour-necrosis-factor)-related apoptosis-inducing ligand] in breast cancer cells [24]. AICAR induces neural stem cell differentiation through the JAK

(Janus kinase)/STAT3 (signal transducer and activator of transcription 3) pathway [25]. In each of these examples, AICAR functions independently of AMPK; however, we have little understanding of alternative AICAR effectors.

Given the opposing roles of AMPK and MondoA in cellular adaptation to intracellular bioenergetic charge, we investigated whether AICAR affected MondoA transcriptional activity. In the present study we show that TXNIP expression is induced by AICAR. The AICAR effect is dependent on MondoA and glucose, but surprisingly is independent of AMPK. Instead, AICAR-dependent stimulation of TXNIP requires its contribution to the intracellular adenine nucleotide pool and is phenocopied by processing of adenosine into adenine nucleotides. Collectively, the present study reveals one mechanism by which AICAR can influence gene expression independent of AMPK and that MondoA regulates target gene expression by sensing intracellular adenine nucleotides.

MATERIALS AND METHODS

Chemicals

AICAR was from Toronto Research Chemicals. 5-Iodotubercidin was from Santa Cruz Biotechnology. Other reagents were from Sigma.

Cell culture

AMPK$\alpha^{+/+}$ and AMPK$\alpha^{-/-}$ (AMPK$\alpha1^{-/-}\alpha2^{-/-}$) MEFs (mouse embryonic fibroblasts) were obtained from Dr Reuben Shaw (Salk Institute for Biological Studies, La Jolla, CA, U.S.A.) [26]. WT (wild-type) and MondoA-KO (knockout) MEFs were generated as described previously [8]. MondoA-KO MEFs were rescued by expressing human MondoA using a retroviral expression system [8]. MEFs and HeLa cells were grown in DMEM (Dulbecco's modified Eagle's medium) with 4.5 g/l glucose, 4 mM glutamine and 2 mM sodium pyruvate (HyClone), supplemented with 0.5% penicillin/streptomycin (Invitrogen) and 10% FBS (fetal bovine serum; HyClone). For glucose-depletion experiments, cells were grown overnight in glucose-free DMEM with glutamine (Invitrogen), supplemented with antibiotics, 10% FBS and 2 mM sodium pyruvate (Invitrogen). The concentrations of glucose indicated in the Figures were added back to the cultures overnight. All cells were maintained at 37°C in 5% CO_2.

Immunoblots

Primary antibodies were used at a dilution of 1:500 for anti-MondoA [7], 1:1000 for anti-VDUP1 (TXNIP) (Medical and Biological Laboratories), 1:10000 for anti-tubulin (Sigma), 1:500 for anti-ADK (Abcam), 1:2000 for anti-ATIC (AICAR formyltransferase/IMP cyclohydrolase; Sigma) and 1:1000 for antibodies against p-AMPKα (p- is phospho), AMPKα, p-S6, S6, p-Raptor and Raptor (Cell Signaling Technology). Secondary antibodies (Amersham Biosciences and R&D Systems) were used at a dilution of 1:5000. Western Lightning Chemiluminescence Plus (PerkinElmer) was used for detection.

qPCR (quantitative real-time PCR)

For expression analysis, 2.5×10^5 cells were incubated overnight on 60 mm dishes, and then treated for 6 h with the reagents indicated in the Figures. Total RNA was extracted using the RNeasy Mini Kit (Qiagen), and cDNA was synthesized from 2 μg of total RNA using the SuperScript III RT system (Invitrogen). qPCR analysis was performed as described previously [5]. Primer sequences are available on request from the corresponding author.

Promoter activity assay

Luciferase reporter assays were performed as described previously [27] following 0.5 mM AICAR treatment for 6 h after overnight transfection.

ChIP (chromatin immunoprecipitation)

ChIP assays were performed as described previously [8] with cells treated with 0.5 mM AICAR for 6 h. Whole-cell lysates were immunoprecipitated with an antibody against MondoA [7]. Co-immunoprecitated DNA was quantified by qPCR with primers specific for the mouse *Txnip* E-box or the *Arrdc4* promoter and normalized to an off-target region. Primer sequences are available on request from the corresponding author.

Gene silencing

For depletion of ADK or ATIC, *Silencer*® Select Negative Control No. 2 siRNA (small interfering RNA; Ambion) as a non-specific control, and mouse ADK or ATIC siRNA (Ambion) were transfected into AMPK$\alpha^{+/+}$ and AMPK$\alpha^{-/-}$ MEFs using Lipofectamine™ RNAiMAX (Invitrogen) according to the manufacturer's protocol. The ADK siRNA sequences were 5′-GCAUUGGGAUAGAUAAGUUTT-3′and 5′-AACUUAUCUAUCCCAAUGCAT-3′, and the ATIC siRNA sequences were 5′-CCAAUGCGAUUGAUCAGUATT-3′and 5′-UACUGAUCAAUCGCAUUGGAG-3′.

Measurement of the ECAR (extracellular acidification rate)

The ECAR of cells were measured using the XF24 Extracellular Flux Analyzer (Seahorse Bioscience). Cells (4×10^4) were incubated overnight on XF24 cell culture microplates (Seahorse Bioscience), and then growth medium was changed for 500 μl of non-buffered DMEM containing 25 mM glucose and 2 mM glutamine (Sigma). Cells were incubated in a CO_2-free incubator at 37 °C for 1 h before loading into the XF24 Analyzer. XF assays were performed by repeating mix (2 min), wait (2 min) and measure (3 min) cycles to determine the ECAR every 7 min. The sequential cycles were continued for 6 h after injection of the compounds indicated.

Analysis of intracellular ATP levels

Quantitative detection of intracellular ATP was performed using the ATP Bioluminescence Assay Kit CLS II (Roche Applied Science) and the GloMax-Multi Detection System (Promega). Cells (1.0×10^5) were incubated overnight on six-well plates, and then treated with 0.5 mM AICAR for the times indicated in the Figures. After removal of culture media, cells were lysed and ATP levels were measured according to the manufacturer's protocol.

Statistical methods

Data represent the mean ± S.E.M. for five biological replicates for ECAR and for three biological replicates for other methods. *P* values were calculated by two-sided Student's *t* tests for two-sampled comparisons. For the experiment examining *Txnip* mRNA levels in AMPK$\alpha^{+/+}$ and AMPK$\alpha^{-/-}$ MEFs, two-way ANOVA models with interaction were fit to log-transformed data.

RESULTS

AICAR up-regulates TXNIP expression in an AMPK-independent manner

To investigate the effects of AICAR on TXNIP expression, MEFs were treated with various concentrations of AICAR (0–1 mM) for 6 h. Since AICAR is an AMPK activator, we determined AMPK-dependence by examining its effects in AMPK$\alpha^{+/+}$ and AMPK$\alpha^{-/-}$ MEFs [26]. TXNIP expression was induced by AICAR treatment at 0.2–0.5 mM in AMPK$\alpha^{+/+}$ MEFs, and this induction was also observed in AMPK$\alpha^{-/-}$ cells (Figure 1A). These low concentrations of AICAR did not change the level of AMPK phosphorylated on Thr^{172} [17], suggesting they were not sufficient to activate AMPK. AICAR treatment at 0.5 mM resulted in a similar increase in *Txnip* mRNA in both cell types, even though *Txnip* mRNA levels in AMPK$\alpha^{-/-}$ were generally slightly lower than in AMPK$\alpha^{+/+}$ MEFs (Figure 1B). This latter finding may explain the generally reduced TXNIP protein levels in AMPK$\alpha^{-/-}$ cells (Figure 1A). Therefore low levels of AICAR stimulateTXNIPtranscriptionindependentofAMPKactivation.

In contrast with low-dose AICAR, TXNIP protein levels were reduced by treatment with 1 mM AICAR, which is sufficient to activate AMPK (Figure 1A). This effect was blunted in AMPK$\alpha^{-/-}$ MEFs, indicating an AMPK-dependent decrease in TXNIP. Thus the response of TXNIP to AICAR is biphasic: low levels of AICAR induce TXNIP expression in an AMPK-independent manner and high levels of AICAR block TXNIP accumulation in an AMPK-dependent manner. Consistent with a second regulatory phase, potent activation of AMPK with metformin, which activates AMPK via inhibition of mitochondrial complex I, also blocked TXNIP expression (Figure 1C).

TXNIP is a negative regulator of glucose metabolism [12,13]. Therefore we examined whether AICAR affected glycolysis by measuring the ECAR. AICAR (at 0.5 mM) decreased the ECAR (Figure 1D), suggesting that AICAR-mediated induction of TXNIP suppressed glycolysis. In contrast, metformin suppressed TXNIP expression and increased the ECAR (Figure 1D). AICAR also induced TXNIP in HeLa cells at concentrations insufficient to stimulate AMPK activity (Figure 1E). These findings show that AICAR induction of TXNIP is not restricted to MEFs and suggest that some aspect(s) of AICAR metabolism, rather than AMPK activation, drives TXNIP expression and restrains glycolysis. In the present study we investigated the AMPK-independent effects of AICAR. In all subsequent experiments, 0.5 mM AICAR was used.

AICAR induces TXNIP expression by enhancing MondoA transcriptional activity

Our previous work demonstrated that MondoA regulates TXNIP expression directly in response to increased glucose levels [5,8,9,16]. Consistent with these findings, AICAR only induced TXNIP expression robustly when the glucose concentration was more than 5 mM (Figure 2A). Thus glucose is required for the AICAR-mediated induction of TXNIP.

To determine whether MondoA was required for AICAR to stimulate TXNIP expression, we used MondoA-KO MEFs lacking exons 12 through 15 of the *Mondoa* gene [8]. Deletion of these exons removes the bHLHZip domain of MondoA and abrogates the transcriptional activity of MondoA [8]. Compared with WT MEFs, TXNIP mRNA and protein were no longer inducible by AICAR in MondoA-KO MEFs (Figures 2B and 2C). Stable transduction of human *MondoA* cDNA into the MondoA-KO MEFs restored basal TXNIP expression and AICAR-mediated TXNIP induction (Figure 2C). Additionally, the activity of a *Txnip* promoter-luciferase reporter was induced by AICAR treatment in WT cells, but not in MondoA-KO cells (Figure 2D). The expression of another known MondoA target, *Arrdc4*, was also induced by AICAR treatment in WT cells, but not in MondoA-KO cells (Figure 2E), indicating that the AICAR effect on MondoA is not restricted to TXNIP. To test whether AICAR regulated MondoA transcriptional activity directly, we examined AICAR-mediated effects on MondoA occupancy on the *Txnip* and *Arrdc4* promoters. MondoA binding to the *Txnip* and *Arrdc4* promoters was increased by AICAR treatment (Figure 2F). These data suggest that AICAR induces TXNIP and ARRDC4 expression by enhancing MondoA promoter occupancy and potentially other steps in transcriptional activation.

AICAR metabolism is required for induction of TXNIP expression

In CHO (Chinese-hamster ovary) cells AICAR, at concentrations similar to those used in the present study, stimulates purine biosynthesis by being metabolized to IMP [28]. IMP enters the purine nucleotide pool [28]; therefore AICAR can be incorporated to the late steps of *de novo* purine biosynthesis by metabolic flux through IMP (Figure 3A). Consistent with previous studies [28,29], intracellular ATP levels increased more than 2-fold following 2 h of AICAR treatment and continued to increase over time (Figure 3B). Thus AICAR contributes to the purine nucleotide pool in MEFs, raising the possibility that AICAR-derived purine nucleotides are involved in the TXNIP induction.

To determine whether AICAR-derived metabolites induced TXNIP, the metabolic processing of AICAR was disrupted at different steps (Figure 3A). We first examined whether AICAR-mediated TXNIP induction depended on AICAR uptake and its phosphorylation to ZMP. Two adenosine transporter inhibitors, NBTI (nitrobenzylthioinosine) and DP (dipyridamole) impaired the AICAR-dependent induction of TXNIP mRNA and protein (Figures 3C and 3D). 5-Iodotubercidin, an inhibitor of ADK, which phosphorylates AICAR to ZMP, also suppressed AICAR-mediated induction of TXNIP mRNA and protein (Figures 3E and 3F). AICAR induction of TXNIP expression was also reduced by transient knockdown of ADK using siRNA (Figure 3G). These data show that uptake and phosphorylation of AICAR to ZMP are required for its induction of TXNIP transcription.

We next examined whether AICAR-mediated TXNIP induction required the conversion of ZMP into IMP, which is the next step in the AICAR metabolic pathway (Figure 3A), by transient knockdown of ATIC using siRNA. ATIC expression levels were reduced significantly 24 h post-transfection of siRNA in AMPK$\alpha^{+/+}$ and AMPK$\alpha^{-/-}$ MEFs (Figure 4A). ATIC siRNA suppressed the AICAR-dependent induction of TXNIP mRNA and protein in AMPK$\alpha^{+/+}$ cells (Figure 4A and 4B respectively). ATIC deficiency leads to ZMP accumulation in cells following AICAR treatment [30], resulting in AMPK activation. Consistent with the accumulation of ZMP, AICAR treatment of ATIC-knockdown cells increased p-AMPK and dramatically reduced p-S6 levels (Figure 4A). This suggests that knockdown of ATIC blocked the conversion of ZMP into IMP allowing ZMP to accumulate to levels sufficient to activate AMPK. To exclude effects on AMPK activation by high ZMP, we also tested whether knockdown of ATIC affected TXNIP induction in AMPK$\alpha^{-/-}$ cells. Knockdown of ATIC also suppressed AICAR-mediated induction of TXNIP protein and mRNA in AMPK$\alpha^{-/-}$ cells (Figures 4A and 4B respectively). Thus the high ectopic levels of ZMP and AMPK activation resulting from knockdown of ATIC do not block TXNIP expression. Rather, these data suggest that the conversion of AICAR into IMP is necessary for induction of TXNIP.

IMP can be hydrolysed to inosine or it can flow into purine nucleotide synthetic pathways, resulting in an increase in ATP and GTP levels [28]. A previous report showed that in HeLa cells a number of adenosine-containing molecules stimulate TXNIP transcription, requiring intracellular Ca^{2+} as a second messenger [31]. We wondered whether AICAR, via entry into purine nucleotide biosynthetic pathways, could induce TXNIP through a similar Ca^{2+}-dependent mechanism. We determined whether intracellular Ca^{2+} was required for AICAR to induce TXNIP by using the cell-permeable Ca^{2+} chelator BAPTA/AM [1,2-bis-(*o*-aminophenoxy)ethane-*N*,*N*,*N*′,*N*′-tetra-acetic acid tetrakis(acetoxymethyl ester)]. In MEFs, BAPTA/AM did not impair induction of TXNIP mRNA or protein by AICAR, adenosine or ATP (Figures 5A and 5B), suggesting that intracellular Ca^{2+} is not required for their induction of TXNIP. In HeLa cells, BAPTA/AM suppressed TXNIP induction by ATP, as reported previously [31], and also suppressed induction by AICAR and adenosine (Figure 5C). We conclude that AICAR, adenosine and ATP can activate TXNIP expression in MEFs by a Ca^{2+}-independent mechanism that is distinct from the previously described [31] Ca^{2+}-dependent mechanism in HeLa cells.

AICAR stimulates TXNIP expression through its metabolism to adenine nucleotides

Because AICAR induced TXNIP independently of Ca^{2+}, we next investigated which IMP-derived metabolite affects MondoA activity by treating control and ATIC-knockdown cells with inosine, guanosine and adenosine. Inosine elevated TXNIP expression, but not to the same level as AICAR (Figure 6A), probably due to conversion of inosine into IMP (Figure 3A). Furthermore, inosine did not induce TXNIP levels in ATIC-knockdown cells (Figure 6A), suggesting that flux of endogenous nucleotides into IMP was required for the modest effect of inosine on TXNIP induction. These data suggest that AICAR flux into inosine is not the primary mechanism by which AICAR affects MondoA activity.

To test whether AICAR-mediated filling of the purine nucleotide pool accounted for TXNIP induction, we determined whether guanosine or adenosine could drive TXNIP induction. Guanosine did not induce TXNIP expression in control and ATIC-knockdown cells (Figure 6B), suggesting that guanosine metabolism does not contribute to AICAR induction. By contrast, adenosine stimulated TXNIP expression to levels similar to those observed with AICAR treatment. Unlike inosine and guanosine, adenosine drove high TXNIP expression in ATIC-knockdown cells (Figure 6C). The ECAR was reduced by adenosine treatment (Figure 1D), which is consistent with high expression of TXNIP. Furthermore, an adenosine transporter inhibitor, DP, suppressed adenosine induction of TXNIP (Figure 6D). Thus adenosine entry into cells, rather than activation of adenosine receptors [32], is required for its stimulation of TXNIP expression. We conclude that intracellular adenosine metabolites are essential for TXNIP induction.

Finally, we examined whether the phosphorylation of adenosine, which generates adenine nucleotides, was necessary for induction of TXNIP expression and whether its effect was transcriptional. Similar to its effect on AICAR-mediated TXNIP induction (Figures 3F and 3G), the ADK inhibitor 5-iodotubercidin or knockdown of ADK restrained adenosine-mediated induction of TXNIP mRNA and protein (Figures 7A, 7B and 3G). 5-Iodotubercidin was less effective at reducing the adenosine-dependent induction of TXNIP in control cells than in ATIC-knockdown cells. This finding may reflect the fact that endogenous IMP can contribute to the purine nucleotide pool in control, but not in ATIC-knockdown, cells. Therefore adenine nucleotides rather than adenosine itself drive the transcriptional induction of TXNIP.

DISCUSSION

MondoA–Mlx complexes are required for approximately 75% of glucose-dependent transcription [5,8], suggesting an important function in nutrient and bioenergetic homoeostasis. Mechanistically, G6P drives the nuclear accumulation, promoter binding and transcriptional activity of MondoA–Mlx complexes [8]. Through their activation of TXNIP and ARRDC4, MondoA– Mlx complexes drive a negative-feedback circuit that further restricts glucose uptake. By dissecting an AICAR-dependent, but AMPK-independent, induction of TXNIP and ARRCD4, we discovered that MondoA–Mlx complexes also respond to adenine nucleotides. We confirmed this model by demonstrating that adenosine could also induce TXNIP expression by a mechanism that required cellular entry and conversion into adenine nucleotides by ADK. In contrast with a previous report in HeLa cells [31], the effects of adenosine on TXNIP expression in MEFs are Ca^{2+}-independent.

At concentrations of AICAR sufficient to activate AMPK, TXNIP expression was down-regulated in a manner that requires AMPK activation. This is consistent with findings of others showing that AMPK activation can down-regulate the transcriptional function of the MondoA paralogue ChREBP (ChoRE-binding protein), at the pyruvate kinase promoter in liver cells and at the *Txnip* promoter in pancreatic β-cells [33,34]. Furthermore, the Cantley laboratory showed recently that TXNIP can be phosphorylated by AMPK, which targets it for degradation [35]. TXNIP degradation adds to the panoply of mechanisms engaged following AMPK activation to restore homoeostasis in response to low bioenergetic charge.

Conceptually, we propose that activation of the MondoA–TXNIP axis is similar to activation of AMPK in that its activation triggers an adaptive programme that allows restoration of metabolic/bioenergetic homoeostasis. However, in contrast with AMPK activation in response to a low bioenergetic charge, our data suggest that MondoA–Mlx complexes sense a high metabolic/bioenergetic state and restrict glucose uptake via the up-regulation of TXNIP and ARRDC4. A restriction of glucose uptake reduces glycolytic flux and flux of glucose-derived carbons into biosynthetic pathways' restoring of metabolic/bioenergetic homoeostasis.

The conversion of AICAR into ZMP activates AMPK, and many of its effects on cell physiology can be attributed to this regulatory circuit [18]. However, several reports suggest that AICAR can also affect a variety of cellular processes independent of AMPK activation. In some cases AICAR-mediated effects require its conversion into ZMP [36], whereas in other cases this metabolism is not required [19,20,22,23]. Most closely related to the present study is the finding in hepatocytes that AICAR, through its conversion into adenine nucleotides, activates the PPARα (peroxisome-proliferator-activated receptor α) target genes *Acox1* (acyl-CoA oxidase 1), *Acadm* (acyl-CoA dehydrogenase, medium chain), *Cpt1a* (carnitine palmitoyltransferase 1a) and *Fabp1* (fatty acid-binding protein 1) [36]. It will be interesting to determine whether adenine nucleotides affected the expression of other MondoA transcriptional targets or whether their effects were restricted to TXNIP and ARRDC4. If so, in addition to its well-characterized effects mediated by AMPK activation [18], AICAR may have broad effects on gene expression by modulating MondoA transcriptional activity.

Several experiments support the hypothesis that MondoA-regulated transcription of the *TXNIP* gene requires adenine nucleotides rather than adenosine. First, a previous study showed that at concentrations similar to those used in the present study, AICAR treatment led to the maximum increase in the purine nucleotide pool [28]. Consistent with this, we observed an increase in ATP levels following AICAR treatment. Secondly, blocking AICAR metabolism at several steps before its entry into the purine nucleotide pool suppressed TXNIP induction. Thirdly, the blockade of AICAR metabolism by knockdown of ATIC could be rescued by the addition of adenosine, but not by the addition of guanosine or inosine. Finally, the effect of adenosine on TXNIP expression was blocked by inhibition of adenosine transport or ADK, suggesting that its stimulation of TXNIP expression requires cellular entry and modification to adenine nucleotides. Therefore we propose that MondoA activates TXNIP expression in response to the level of intracellular adenine nucleotides, which can be derived from AICAR or adenosine. Given the intra-conversion of AMP, ADP and ATP *in vivo* [37], we do not yet know which adenine nucleotide is sensed by MondoA.

A previous report indicated that adenosine-containing molecules, e.g. NAD^+, NAD, FAD and cAMP, activate TXNIP transcription [31]. In HeLa cells, the cell-permeable Ca^{2+} chelator BAPTA/AM blocks TXNIP transcriptional activation in response to ATP, NADH and NAD^+, implying that adenosine-containing molecules trigger mobilization of Ca^{2+} stores to stimulate MondoA–Mlx transcriptional activity. In contrast, in our MEF system, BAPTA/AM increased basal TXNIP expression and did not affect TXNIP expression induced by AICAR, adenosine or ATP. We observed the same effects of BAPTA/AM on

TXNIP induction in HeLa cells as reported previously [31]. Our studies in MEFs suggest that adenine nucleotides themselves, and not Ca^{2+} mobilization, stimulate MondoA transcriptional activity at the *Txnip* promoter. Thus MondoA can activate TXNIP expression by Ca^{2+}-dependent (HeLa) and independent (MEFs) mechanisms. Similar to our findings in MEFs, TXNIP is also induced by AICAR in a human pancreatic cancer cell line, BxPC3, independent of AMPK activation and Ca^{2+} (M.R. Kaadige and D.E. Ayer, unpublished work). In contrast, we observed no TXNIP induction by AICAR in immortal diploid human fibroblasts (M.R. Kaadige and D.E. Ayer, unpublished work). Thus the Ca^{2+}-independent induction of TXNIP by low-dose AICAR is not restricted to mouse cells or fibroblasts. Finally, in our experiments (Figure 5) and in those from the Luo group [31], BAPTA/AM treatment increased basal TXNIP mRNA and protein levels. Thus a more general Ca^{2+}-dependent repression mechanism may also control TXNIP expression under basal growth conditions. Alternatively, reduction in intracellular Ca^{2+} by BAPTA/AM may be sensed as a cellular stress and induce TXNIP by an indirect mechanism. Additional experiments are required to elucidate the determinants of Ca^{2+}-dependent and -independent TXNIP induction in response to adenosine-containing molecules and how Ca^{2+} controls TXNIP expression under basal growth conditions.

Several mechanisms may explain how adenine nucleotides can activate *TXNIP* gene expression. First, G6P is essential for MondoA transcriptional activity [5,8]. Glucose and ATP are required to generate G6P and glucose is required for AICAR to stimulate TXNIP expression. In the present study, AICAR (Figure 3B) or adenosine (results not shown) increased intracellular ATP levels. Thus it is conceivable that intracellular ATP levels help determine the levels of G6P. Supporting this model is the finding that increasing ATP levels stimulate the enzymatic activity of hexokinase, which catalyses conversion of glucose into G6P [38]. Secondly, ATP levels are linked to mitochondrial membrane potential [39], raising the possibility that the regulation by MondoA of TXNIP expression may be tied to mitochondrial function. Supporting this hypothesis, we observed that metformin and oligomycin, which inhibit the mitochondrial electron transport chain, restrained AICAR or adenosine from inducing TXNIP expression and decreased intracellular ATP levels (results not shown). Furthermore, a previous study reported that OXPHOS inhibitors down-regulate TXNIP expression [40], and we observed a reduction in TXNIP expression in rho° cells which lack mitochondrial DNA and cannot perform OXPHOS (M.R. Kaadige and D.E. Ayer, unpublished work). Finally, high intracellular ATP levels decrease glycolytic rate by allosteric inhibition of PFK-1 (phosphofructokinase-1), one of the important regulatory enzymes of glycolysis [41,42]. Reduction of glycolysis could lead to G6P accumulation and trigger MondoA transcriptional activity.

Further experiments are needed to determine the precise molecular mechanism(s) by which MondoA responds to adenine nucleotides. Nonetheless the present study indicates that MondoA, by sensing G6P and adenine nucleotides, allows cells to adapt to a high metabolic or bioenergetic state. However, the transcriptional activity of MondoA at the *TXNIP* promoter is under the control of a number of other metabolites, e.g. α-oxoglutarate [9], lactate and protons [43]. We suggest a broad role for MondoA in sensing and integrating

information about the changing concentrations of cellular metabolites, ultimately driving adaptive transcriptional responses to maintain metabolic homoeostasis.

ACKNOWLEDGEMENTS

We thank Dr Reuben Shaw for AMPK$\alpha^{+/+}$ and AMPK$\alpha^{-/-}$ MEFs, Jamie Soto in the Metabolic Phenotyping Core facility for operation of the XF24 analyser, Ken Boucher for statistical analysis, Mohan Kaadige, John O'Shea and Elizabeth Leibold for review of the paper before submission, and members of the Ayer laboratory for insightful discussion.

FUNDING

This work was supported by the National Institutes of Health [grant numbers GM55668, DK084425 (to D.E.A.)] and the Huntsman Cancer Foundation. DNA sequencing and oligonucleotide synthesis were supported by a Cancer Center Support Grant [grant number 2P30 CA42014].

Abbreviations used

ADK	adenosine kinase
AICAR	5-amino-4-imidazolecarboxamide ribofuranoside
AMPK	AMP-activated protein kinase
ARRDC4	arrestin domain-containing protein 4
ATIC	AICAR formyltransferase/IMP cyclohydrolase
BAPTA/AM	1,2-bis-(*o*-aminophenoxy)ethane-*N*,*N*,*N*′,*N*′-tetra-acetic acid tetrakis(acetoxymethyl ester)
bHLHZip	basic helix–loop–helix leucine zipper
ChIP	chromatin immunoprecipitation
ChoRE	carbohydrate-response element
DMEM	Dulbecco's modified Eagle's medium
DP	dipyridamole
ECAR	extracellular acidification rate
FBS	fetal bovine serum
G6P	glucose 6-phosphate
KO	knockout
MEF	mouse embryonic fibroblast
NBTI	nitrobenzylthioinosine
OMM	outer mitochondrial membrane
OXPHOS	oxidative phosphorylation
qPCR	quantitative real-time PCR
siRNA	small interfering RNA

TXNIP	thioredoxin-interacting protein
WT	wild-type
ZMP	5-amino-4-imidazolecarboxamide ribonucleotide

REFERENCES

1. Howell JJ, Manning BD. mTOR couples cellular nutrient sensing to organismal metabolic homeostasis. Trends Endocrinol. Metab. 2011; 22:94–102. [PubMed: 21269838]
2. Vander Heiden MG, Cantley LC, Thompson CB. Understanding the Warburg effect: the metabolic requirements of cell proliferation. Science. 2009; 324:1029–1033. [PubMed: 19460998]
3. Herman MA, Kahn BB. Glucose transport and sensing in the maintenance of glucose homeostasis and metabolic harmony. J. Clin. Invest. 2006; 116:1767–1775. [PubMed: 16823474]
4. Warburg O. On the origin of cancer cells. Science. 1956; 123:309–314. [PubMed: 13298683]
5. Stoltzman CA, Peterson CW, Breen KT, Muoio DM, Billin AN, Ayer DE. Glucose sensing by MondoA:Mlx complexes: a role for hexokinases and direct regulation of thioredoxin-interacting protein expression. Proc. Natl. Acad. Sci. U.S.A. 2008; 105:6912–6917. [PubMed: 18458340]
6. Billin AN, Eilers AL, Coulter KL, Logan JS, Ayer DE. MondoA, a novel basic helix-loop-helix-leucine zipper transcriptional activator that constitutes a positive branch of a max-like network. Mol. Cell. Biol. 2000; 20:8845–8854. [PubMed: 11073985]
7. Sans CL, Satterwhite DJ, Stoltzman CA, Breen KT, Ayer DE. MondoA-Mlx heterodimers are candidate sensors of cellular energy status: mitochondrial localization and direct regulation of glycolysis. Mol. Cell. Biol. 2006; 26:4863–4871. [PubMed: 16782875]
8. Peterson CW, Stoltzman CA, Sighinolfi MP, Han KS, Ayer DE. Glucose controls nuclear accumulation, promoter binding, and transcriptional activity of the MondoA-Mlx heterodimer. Mol. Cell. Biol. 2010; 30:2887–2895. [PubMed: 20385767]
9. Kaadige MR, Looper RE, Kamalanaadhan S, Ayer DE. Glutamine-dependent anapleurosis dictates glucose uptake and cell growth by regulating MondoA transcriptional activity. Proc. Natl. Acad. Sci. U.S.A. 2009; 106:14878–14883. [PubMed: 19706488]
10. Nishiyama A, Matsui M, Iwata S, Hirota K, Masutani H, Nakamura H, Takagi Y, Sono H, Gon Y, Yodoi J. Identification of thioredoxin-binding protein-2/vitamin D3 up-regulated protein 1 as a negative regulator of thioredoxin function and expression. J. Biol. Chem. 1999; 274:21645–21650. [PubMed: 10419473]
11. Kim SY, Suh HW, Chung JW, Yoon SR, Choi I. Diverse functions of VDUP1 in cell proliferation, differentiation, and diseases. Cell. Mol. Immunol. 2007; 4:345–351. [PubMed: 17976314]
12. Parikh H, Carlsson E, Chutkow WA, Johansson LE, Storgaard H, Poulsen P, Saxena R, Ladd C, Schulze PC, Mazzini MJ, et al. TXNIP regulates peripheral glucose metabolism in humans. PLoS Med. 2007; 4:e158. [PubMed: 17472435]
13. Patwari P, Chutkow WA, Cummings K, Verstraeten VL, Lammerding J, Schreiter ER, Lee RT. Thioredoxin-independent regulation of metabolism by the α-arrestin proteins. J. Biol. Chem. 2009; 284:24996–25003. [PubMed: 19605364]
14. Minn AH, Hafele C, Shalev A. Thioredoxin-interacting protein is stimulated by glucose through a carbohydrate response element and induces β-cell apoptosis. Endocrinology. 2005; 146:2397–2405. [PubMed: 15705778]
15. Elgort MG, O'Shea JM, Jiang Y, Ayer DE. Transcriptional and translational downregulation of thioredoxin interacting protein is required for metabolic reprogramming during G1. Genes Cancer. 2010; 1:893–907. [PubMed: 21779470]
16. Stoltzman CA, Kaadige MR, Peterson CW, Ayer DE. MondoA senses non-glucose sugars: regulation of thioredoxin-interacting protein (TXNIP) and the hexose transport curb. J. Biol. Chem. 2011; 286:38027–38034. [PubMed: 21908621]
17. Hardie DG. Sensing of energy and nutrients by AMP-activated protein kinase. Am. J. Clin. Nutr. 2011; 93:891S–896S. [PubMed: 21325438]

18. Corton JM, Gillespie JG, Hawley SA, Hardie DG. 5-Aminoimidazole-4-carboxamide ribonucleoside. A specific method for activating AMP-activated protein kinase in intact cells? Eur. J. Biochem. 1995; 229:558–565. [PubMed: 7744080]
19. Jhun BS, Jin Q, Oh YT, Kim SS, Kong Y, Cho YH, Ha J, Baik HH, Kang I. 5-Aminoimidazole-4-carboxamide riboside suppresses lipopolysaccharide-induced TNF-α production through inhibition of phosphatidylinositol 3-kinase/Akt activation in RAW 264.7 murine macrophages. Biochem. Biophys. Res. Commun. 2004; 318:372–380. [PubMed: 15120611]
20. Kuo CL, Ho FM, Chang MY, Prakash E, Lin WW. Inhibition of lipopolysaccharide-induced inducible nitric oxide synthase and cyclooxygenase-2 gene expression by 5-aminoimidazole-4-carboxamide riboside is independent of AMP-activated protein kinase. J. Cell. Biochem. 2008; 103:931–940. [PubMed: 17615555]
21. Labuzek K, Liber S, Gabryel B, Okopien B. AICAR (5-aminoimidazole-4-carboxamide-1-β-4-ribofuranoside) increases the production of toxic molecules and affects the profile of cytokines release in LPS-stimulated rat primary microglial cultures. Neurotoxicology. 2010; 31:134–146. [PubMed: 19853624]
22. Lopez JM, Santidrian AF, Campas C, Gil J. 5-Aminoimidazole-4-carboxamide riboside induces apoptosis in Jurkat cells, but the AMP-activated protein kinase is not involved. Biochem. J. 2003; 370:1027–1032. [PubMed: 12452797]
23. Santidrian AF, Gonzalez-Girones DM, Iglesias-Serret D, Coll-Mulet L, Cosialls AM, de Frias M, Campas C, Gonzalez-Barca E, Alonso E, Labi V, et al. AICAR induces apoptosis independently of AMPK and p53 through up-regulation of the BH3-only proteins BIM and NOXA in chronic lymphocytic leukemia cells. Blood. 2010; 116:3023–3032. [PubMed: 20664053]
24. Garcia-Garcia C, Fumarola C, Navaratnam N, Carling D, Lopez-Rivas A. AMPK-independent down-regulation of cFLIP and sensitization to TRAIL-induced apoptosis by AMPK activators. Biochem. Pharmacol. 2010; 79:853–863. [PubMed: 19896469]
25. Zang Y, Yu LF, Pang T, Fang LP, Feng X, Wen TQ, Nan FJ, Feng LY, Li J. AICAR induces astroglial differentiation of neural stem cells via activating the JAK/STAT3 pathway independently of AMP-activated protein kinase. J. Biol. Chem. 2008; 283:6201–6208. [PubMed: 18077446]
26. Gwinn DM, Shackelford DB, Egan DF, Mihaylova MM, Mery A, Vasquez DS, Turk BE, Shaw RJ. AMPK phosphorylation of raptor mediates a metabolic checkpoint. Mol. Cell. 2008; 30:214–226. [PubMed: 18439900]
27. Billin AN, Eilers AL, Queva C, Ayer DE. Mlx, a novel Max-like BHLHZip protein that interacts with the Max network of transcription factors. J. Biol. Chem. 1999; 274:36344–36350. [PubMed: 10593926]
28. Sabina RL, Patterson D, Holmes EW. 5-Amino-4-imidazolecarboxamide riboside (Z-riboside) metabolism in eukaryotic cells. J. Biol. Chem. 1985; 260:6107–6114. [PubMed: 3997815]
29. Menze MA, Chakraborty N, Clavenna M, Banerjee M, Liu XH, Toner M, Hand SC. Metabolic preconditioning of cells with AICAR-riboside: improved cryopreservation and cell-type specific impacts on energetics and proliferation. Cryobiology. 2010; 61:79–88. [PubMed: 20510224]
30. Marie S, Heron B, Bitoun P, Timmerman T, Van Den Berghe G, Vincent MF. AICA-ribosiduria: a novel, neurologically devastating inborn error of purine biosynthesis caused by mutation of ATIC. Am. J. Hum. Genet. 2004; 74:1276–1281. [PubMed: 15114530]
31. Yu FX, Goh SR, Dai RP, Luo Y. Adenosine-containing molecules amplify glucose signaling and enhance txnip expression. Mol. Endocrinol. 2009; 23:932–942. [PubMed: 19246513]
32. Fields RD, Burnstock G. Purinergic signalling in neuron-glia interactions. Nat. Rev. Neurosci. 2006; 7:423–436. [PubMed: 16715052]
33. Kawaguchi T, Osatomi K, Yamashita H, Kabashima T, Uyeda K. Mechanism for fatty acid “sparing” effect on glucose-induced transcription: regulation of carbohydrate-responsive element-binding protein by AMP-activated protein kinase. J. Biol. Chem. 2002; 277:3829–3835. [PubMed: 11724780]
34. Shaked M, Ketzinel-Gilad M, Cerasi E, Kaiser N, Leibowitz G. AMP-activated protein kinase (AMPK) mediates nutrient regulation of thioredoxin-interacting protein (TXNIP) in pancreatic β-cells. PLoS ONE. 2011; 6:e28804. [PubMed: 22194917]

35. Wu N, Zheng B, Shaywitz A, Dagon Y, Tower C, Bellinger G, Shen CH, Wen J, Asara J, McGraw TE, et al. AMPK-dependent degradation of TXNIP upon energy stress leads to enhanced glucose uptake via GLUT1. Mol. Cell. 2013; 49:1167–1175. [PubMed: 23453806]

36. Bumpus NN, Johnson EF. 5-Aminoimidazole-4-carboxyamide-ribonucleoside (AICAR)-stimulated hepatic expression of Cyp4a10, Cyp4a14, Cyp4a31, and other peroxisome proliferator-activated receptor α-responsive mouse genes is AICAR 5′-monophosphate-dependent and AMP-activated protein kinase-independent. J. Pharmacol. Exp. Ther. 2011; 339:886–895. [PubMed: 21896918]

37. Barkulis SS, Lehninger AL. Myokinase and the adenine nucleotide specificity in oxidative phosphorylations. J. Biol. Chem. 1951; 190:339–344. [PubMed: 14841182]

38. Wilson JE. Isozymes of mammalian hexokinase: structure, subcellular localization and metabolic function. J. Exp. Biol. 2003; 206:2049–2057. [PubMed: 12756287]

39. Brand MD, Nicholls DG. Assessing mitochondrial dysfunction in cells. Biochem. J. 2011; 435:297–312. [PubMed: 21726199]

40. Yu FX, Chai TF, He H, Hagen T, Luo Y. Thioredoxin-interacting protein (Txnip) gene expression: sensing oxidative phosphorylation status and glycolytic rate. J. Biol. Chem. 2010; 285:25822–25830. [PubMed: 20558747]

41. Sola-Penna M, Da Silva D, Coelho WS, Marinho-Carvalho MM, Zancan P. Regulation of mammalian muscle type 6-phosphofructo-1-kinase and its implication for the control of the metabolism. IUBMB Life. 2010; 62:791–796. [PubMed: 21117169]

42. Dunaway GA, Kasten TP, Sebo T, Trapp R. Analysis of the phosphofructokinase subunits and isoenzymes in human tissues. Biochem. J. 1988; 251:677–683. [PubMed: 2970843]

43. Chen JL, Merl D, Peterson CW, Wu J, Liu PY, Yin H, Muoio DM, Ayer DE, West M, Chi JT. Lactic acidosis triggers starvation response with paradoxical induction of TXNIP through MondoA. PLoS Genet. 2010; 6:e1001093. [PubMed: 20844768]

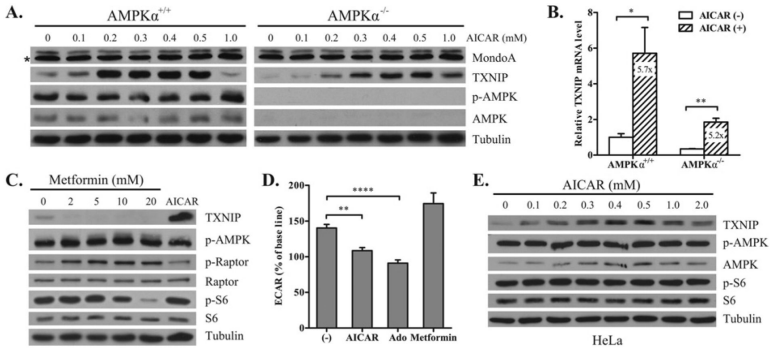

Figure 1. Low levels of AICAR up-regulate TXNIP transcription

(**A** and **E**) Levels of the proteins indicated were determined by Western blotting analysis in AMPK$\alpha^{+/+}$ or AMPK$\alpha^{-/-}$ MEFs (**A**) or in HeLa cells (**E**) following a 6 h treatment with the indicated concentrations of AICAR (*non-specific band). (**B**) *Txnip* mRNA levels were determined by qPCR in AMPK$\alpha^{+/+}$ or AMPK$\alpha^{-/-}$ MEFs treated with 0.5 mM AICAR for 6 h. *Txnip* mRNA levels were normalized to *Actb* (β-actin) mRNA levels and results are the fold change relative to the mRNA level in untreated AMPK$\alpha^{+/+}$ cells. The numbers indicate the fold-increase associated with AICAR treatment in each cell population (n =3; *P <0.05 and **P <0.01; the fold-increase in AMPK$\alpha^{+/+}$ or AMPK$\alpha^{-/-}$ cells is not significantly different). (**C**) Levels of the proteins indicated were determined by Western blotting analysis in AMPK$\alpha^{+/+}$ MEFs treated with the indicated concentrations of metformin for 6 h. The effect of metformin was compared with that of 0.5 mM AICAR. (**D**) The ECAR of AMPK$\alpha^{+/+}$ MEFs was measured for 6 h following injection of 0.5 mM AICAR, 0.2 mM adenosine or 5 mM metformin. ECARs were normalized to total protein and data presented as the percentage of the final value (6 h) to initial value (0 h) (n =5; **P <0.01 and ****P <0.0001).

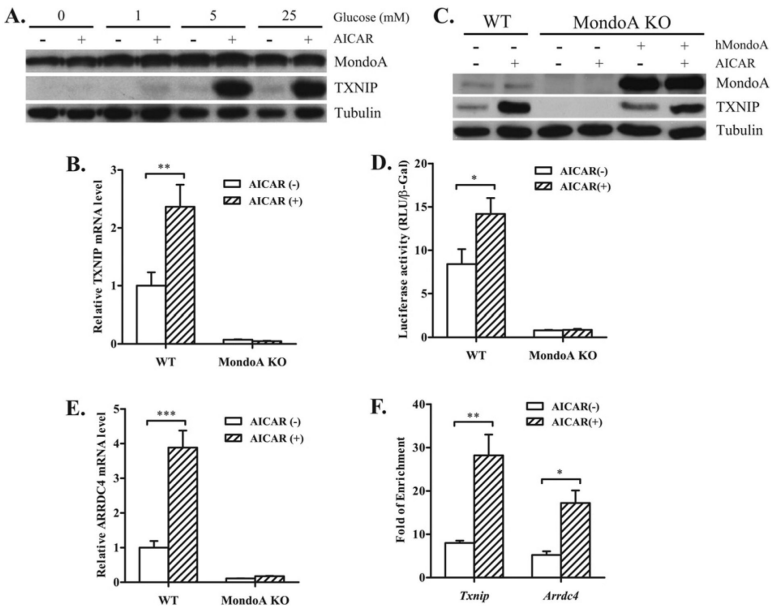

Figure 2. AICAR induces TXNIP expression by enhancing glucose-dependent MondoA transcriptional activity

(**A** and **C**) Levels of the proteins indicated were determined by Western blotting analysis. In (**A**), MEFs were grown overnight in medium containing the indicated concentrations of glucose followed by 0.5 mM AICAR treatment for 6 h. In (**C**), WT or MondoA-KO MEFs and MondoA-KO MEFs complemented with stable transduction of human MondoA were treated with 0.5 mM AICAR for 6 h. (**B** and **E**) *Txnip* (**B**) or *Arrdc4* (**E**) mRNA levels were determined by qPCR and normalized to *Actb* (*β*-actin) expression following 0.5 mM AICAR treatment for 6 h. Results are the fold change relative to the mRNA level in untreated WT cells. (**D**) *Txnip* promoter activity was examined using a luciferase reporter assay following 6 h of AICAR treatment. (**F**) Occupancy of MondoA at the *Txnip* and *Arrdc4* promoters was determined by ChIP in MEFs treated with 0.5 mM AICAR for 6 h (n =3). *P <0.05, **P <0.01 and ***P <0.001.

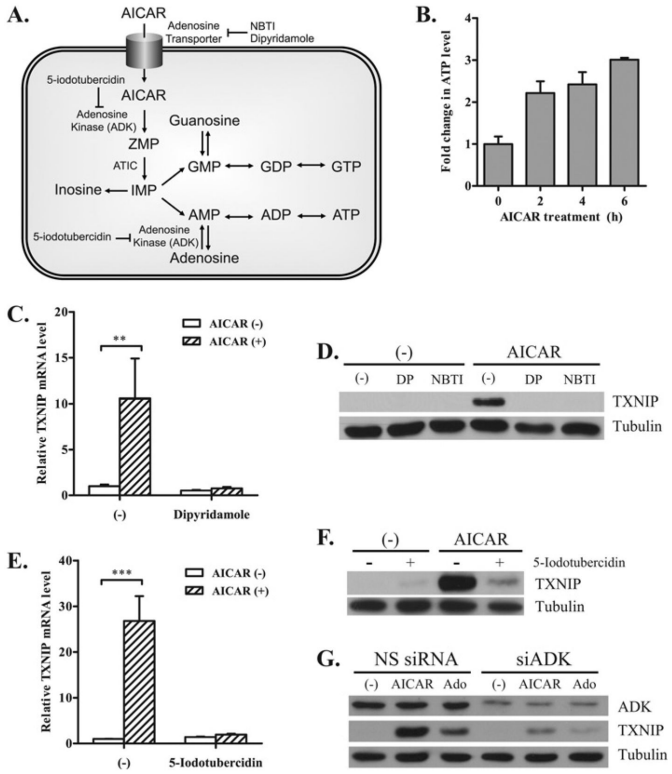

Figure 3. AICAR increases intracellular ATP levels, and its metabolism to ZMP is required for TXNIP induction

(**A**) The AICAR metabolic pathway. AICAR enters cells through adenosine transporters and is metabolized to ZMP by ADK. ZMP is metabolized to IMP by ATIC. IMP enters the purine nucleotide pool, ultimately being metabolized to GMP and AMP. IMP can also be metabolized to inosine. NBTI and DP are adenosine transporter inhibitors and 5-iodotubercidin is an ADK inhibitor. (**B**) Intracellular ATP levels were determined in MEFs treated with 0.5 mM AICAR for the times indicated. ATP levels were normalized to total protein and results are the fold change relative to the ATP level in untreated cells. (**C** and **E**) *Txnip* mRNA levels were determined by qPCR and normalized to Actb (β-actin) expression. Results are the fold change relative to the mRNA level in untreated cells (n =3; $^{**}P$ <0.01 and $^{***}P$ <0.001). (**D** and **F**) Levels of the proteins indicated were determined by Western blotting analysis. MEFs were incubated for 6 h following the addition of 0.5 mM AICAR with DP (10 μM), NBTI (20 μM) or 5-iodotubercidin (0.5 μM). (**G**) Levels of the proteins indicated were determined by Western blotting analysis in MEFs transfected with ADK siRNA or non-specific siRNA (NS) following 6 h treatments of AICAR (0.5 mM) or adenosine (Ado, 0.2 mM).

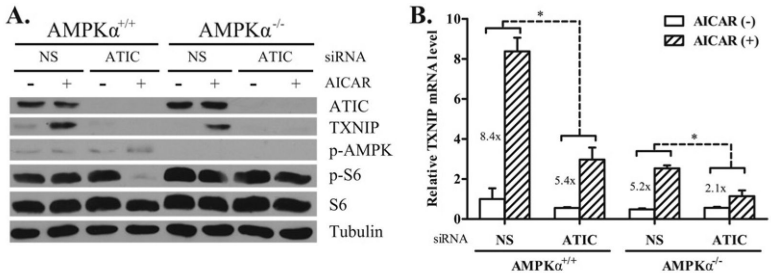

Figure 4. Conversion of AICAR into IMP is necessary for AICAR-mediated TXNIP induction

AMPK$\alpha^{+/+}$ and AMPK$\alpha^{-/-}$ MEFs transfected with siRNA against ATIC or negative control (NS) were treated with 0.5 mM AICAR for 6 h. (**A**) Levels of the proteins indicated were determined by Western blotting analysis. (**B**) *Txnip* mRNA levels were determined by qPCR and normalized to Actb (β-actin) mRNA levels. Results are the fold change relative to the mRNA level in untreated AMPK$\alpha^{+/+}$ cells. The numbers indicate the fold-increase associated with 0.5 mM AICAR treatment in each cell population (n =3; *P <0.05; broken lines indicate the comparisons of the fold increases between negative control and ATIC-knockdown cells; the fold changes in AMPK$\alpha^{+/+}$ or AMPK$\alpha^{-/-}$ MEFs are not significantly different).

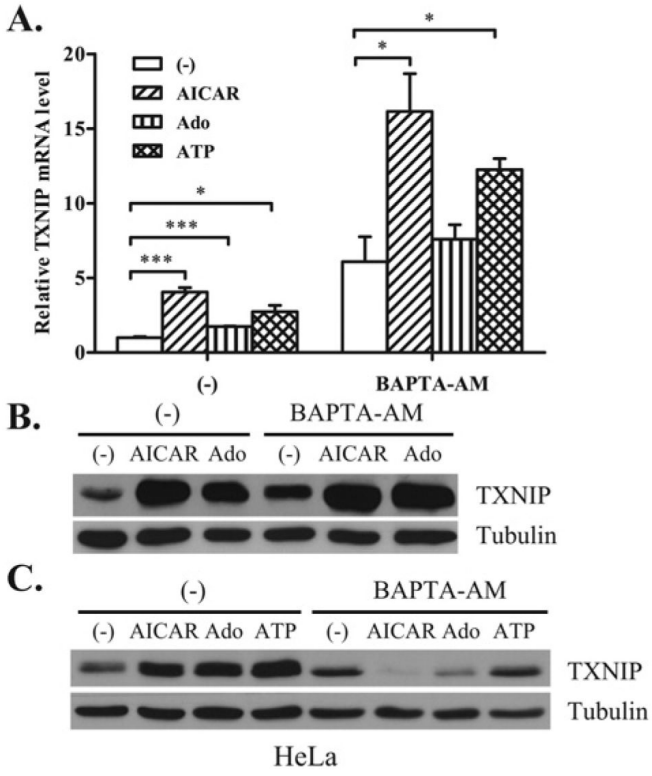

Figure 5. AICAR-mediated induction of TXNIP does not depend on intracellular Ca^{2+} in MEFs

(**A**) *Txnip* mRNA levels were measured by qPCR and normalized to *Actb* (*β*-actin) mRNA levels. Results are the fold change relative to the mRNA level in untreated cells (n =3; **P* <0.05 and ****P* <0.001). (**B** and **C**) Levels of the proteins indicated were determined by Western blotting analysis. MEFs (**A** and **B**) or HeLa cells (**C**) were incubated for 6 h with AICAR (0.5 mM), adenosine (Ado, 0.2 mM) or ATP (0.2 mM) with a cell-permeable Ca^{2+} chelator BAPTA/AM (10 *μ*M).

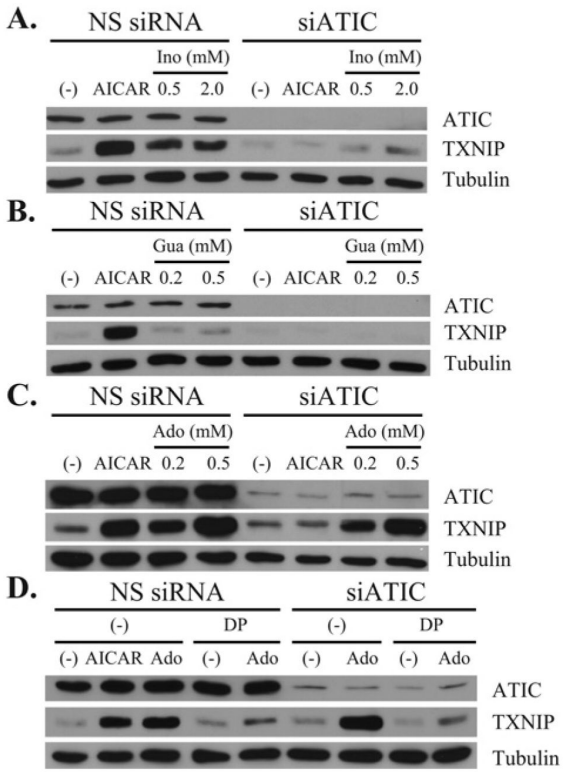

Figure 6. AICAR-derived adenosine induces TXNIP expression

Levels of the proteins indicated were determined by Western blotting analysis. (**A**–**C**) Control (NS) or ATIC-knockdown MEFs were treated with the indicated concentrations of (**A**) inosine (Ino), (**B**) guanosine (Gua) or (**C**) adenosine (Ado) for 6 h. Effects of the nucleosides were compared with 0.5 mM AICAR. (**D**) Control or ATIC-knockdown MEFs were treated with 0.5 mM AICAR or 0.2 mM adenosine (Ado) with an adenosine transporter inhibitor DP (10 μM) for 6 h.

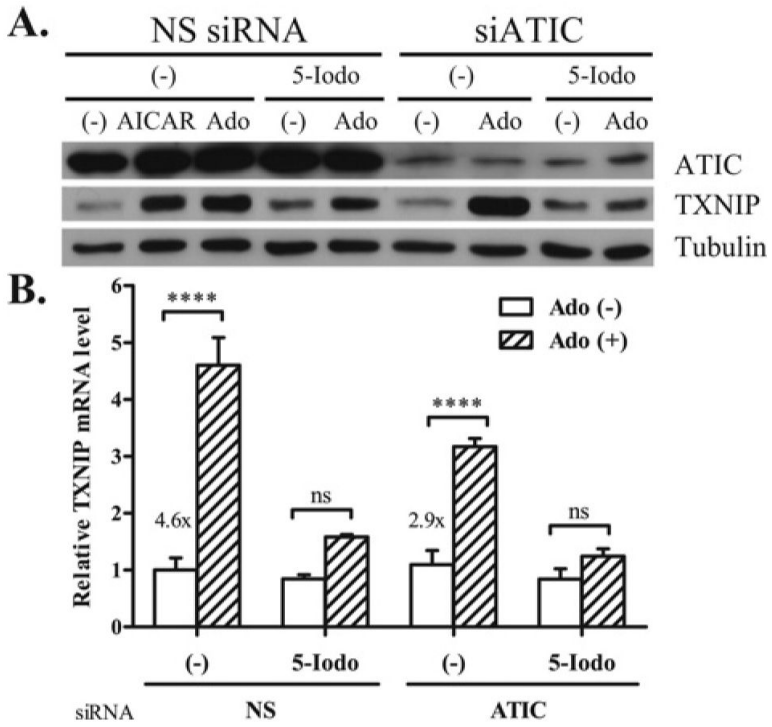

Figure 7. Phosphorylation of adenosine is required for induction of TXNIP expression

(**A**) Levels of the proteins indicated were determined by Western blotting analysis. (**B**) *Txnip* mRNA levels were measured by qPCR and normalized to Actb (β-actin) mRNA levels. Results are the fold change relative to the mRNA level in untreated control cells. The numbers indicate the fold increase associated with 0.2 mM adenosine (Ado) treatment in each cell population (n =3; ns, not significant and ****P <0.0001). Control (NS) or ATIC-knockdown MEFs were treated with 0.5 mM AICAR or 0.2 mM adenosine with an ADK inhibitor 5-iodotubercidin (5-Iodo, 0.5 μM) for 6 h.